Chemistry Europe
European Chemical Societies Publishing

WILEY VCH

Excellence in Chemistry Research

Announcing our new flagship journal

- Gold Open Access
- Publishing charges waived
- Preprints welcome
- Edited by active scientists

Meet the Editors of *ChemistryEurope*

Luisa De Cola
Università degli Studi di Milano Statale, Italy

Ive Hermans
University of Wisconsin-Madison, USA

Ken Tanaka
Tokyo Institute of Technology, Japan

ChemCatChem

Research Article
doi.org/10.1002/cctc.202201408

Chemistry Europe
European Chemical Societies Publishing

www.chemcatchem.org

Hydrogenation of CO_2 into Formates by Ligand-Capped Palladium Heterogeneous Catalysts

M. Dolores Fernández-Martínez[a] and Cyril Godard*[a]

The synthesis of two series of catalysts based on ligand-capped supported Pd nanoparticles was carried out using a simple procedure and the resulting materials were tested in the formate synthesis. Within these series, PPh_3 revealed the most appropriate stabilizing ligand while TiO_2 was the most efficient support for these catalysts. The hydrogenation of CO_2 was carried out under mild reaction conditions (1.8 MPa CO_2, 1.8 MPa H_2, 60 °C) using water as solvent and in the presence of a base, providing excellent selectivity towards formates with a TON of 1032 (TOF of 69 h^{-1}, [HCOOK] = 1.1 mol/l).

Introduction

The environmental issues arising from the high concentration of CO_2 in the atmosphere are nowadays regarded as critical and have triggered much interest in research towards the development of non-fossil-based feedstocks. In this context, despite its inertness, CO_2 has become a very attractive C1 source to obtain fuels and chemicals.[1] However, commercially, the transformation of CO_2 into chemicals is currently limited to the production of urea,[2] polycarbonates,[3] salicylic acid,[4] methanol[1c,5,6,7,8] and carboxylic acids.[9] Among the potential transformations of CO_2, its hydrogenation into formic acid and derivatives have become a priority in view of the recent progress made in the production of H_2 via water splitting.[10] Indeed, formic acid presents high hydrogen storage capacity and stability and provides a way to store CO_2 in a chemically stable form, giving rise to CO_2 mediated hydrogen energy cycle.[11] However, the harsh conditions usually required made the design of efficient and reusable catalysts for this transformation very challenging.

For the transformation of CO_2 into formic acid/formates,[12] several highly active homogeneous catalysts were described.[13] On the other hand, heterogenized[14] and heterogeneous[15] catalysts are usually less active but provide advantages in term of handling and separation for subsequent recycling and reuse. However, if the reaction is performed in the gas phase, high temperatures are usually required and the most interesting products such as HCOOH and MeOH are thermodynamically disfavored.[16] In aqueous phase, the reaction becomes slightly exothermic due to solvation effects and is even more favorable under alkaline conditions. In this process, the pH is a crucial parameter due to the low solubility of CO_2 in water, the type of base used, the temperature and the pressure of CO_2 and H_2. The hydrogenation of CO_2 under basic conditions or from the hydrogenation of carbonates or bicarbonates has several advantages over the HCO_2H/CO_2 system since it allows the release of H_2 without producing CO. The heterogeneous process involves the adsorption and activation of HCO_3^-/CO_2 in solution, the adsorption and dissociation of H_2 and the formation and desorption of formate over the catalyst, which in turn are mainly dependent on the number of catalytic active sites, the electron density at the metal and the interactions between active sites and chemical intermediates. As a result, it was reported that the particle size of the catalysts and the electron density at the metal are key factors for the activity in this reaction.[17] Among the metals reported, Pd was described as one of the most active metals for the production of formic acid/formate[11b,18] and the combination of Pd with other metals such as Au,[11c,19] Ag,[20] and Ni also revealed efficient for this transformation.[21] The choice of the support in this reaction is also important and for instance, Pd catalysts on carbon based supports such as reduced graphene oxide (*r*GO), N-doped carbon (N–C) or mesoporous graphitic carbon nitride (g-C_3N_4) revealed very efficient for the hydrogenation of bicarbonates to formates.[19,22] In 2018, Mori et al. reported the highly efficient CO_2 hydrogenation using Pd based catalysts supported onto TiO_2.[23] In this study, they showed that using bimetallic Pd/Ag nanoparticles, isolated and electron-rich Pd atoms are created and enhance the electronegativity of the dissociated hydride species, resulting in superior catalytic performance.

In this work, the preparation of heterogeneous CO_2 hydrogenation catalysts based on palladium nanoparticles supported on TiO_2 is reported. The decomposition of an organometallic precursor was performed under H_2 in the presence of various ligand stabilizers to control the surface composition and the size of the nanoparticles. Indeed, comparison with other methods such as chemical reduction or wetness impregnation-reduction, this organometallic approach initially developed by Philippot and Chaudret, yields nanoparticles with a clean

[a] M. D. Fernández-Martínez, Dr. C. Godard
Universitat Rovira i Virgili
Departament de Química Física i Inorgànica
Campus Sescelades, C/Marcel·lí Domingo s/n
43007, Tarragona (Spain)
E-mail: cyril.godard@urv.cat

Supporting information for this article is available on the WWW under https://doi.org/10.1002/cctc.202201408

This publication is part of a Special Collection with all Chemistry Europe journals on the "International Symposium on Homogeneous Catalysis". Please follow the link for more articles in the collection.

surface that do not require activation at high temperature.[24,25] Here, phosphorus based ligands and a N-heterocyclic carbene were used as capping agents for Pd nanoparticles and the effect on their catalytic performance in the hydrogenation of CO_2 into formate was particularly looked at.

Results and Discussion

Colloidal and supported Pd nanoparticles were synthesized in THF by decomposition of $Pd(dba)_2$ under 3 bar of H_2 at 60 °C in the presence of 0.2 equivalent of ligand (0.1 eq. in the case of bidentate ligand, 0.5 equivalent for NHC ligand) and the support. The general procedure is described in Scheme 1.

First, the effect of the ligands on the properties of the resulting nanoparticles such as size, dispersion and morphology were evaluated using TiO_2 as support. Various phosphines were used such as triphenylphosphine (PPh_3),[26] which was previously reported as an essential additive for the reduction of CO_2 to FA with heterogeneous catalyst,[17b,27] diphenyl-2-pyridylphosphine (PPh_2Py) and water soluble phosphines such as 1,3,5-triaza-7-phosphaadamantane (PTA) and 3-(diphenylphosphino) benzenesulfonic acid sodium salt (TPPMS) that were previously reported using molecular catalysts.[28,29] The N-heterocyclic carbene (NHC) precursor 1,3-dimethylimidazolium-2-carboxylate ($Me_2Im–CO_2$), previously utilized by our group for the synthesis of mono- and bimetallic nanoparticles,[30] was also tested.

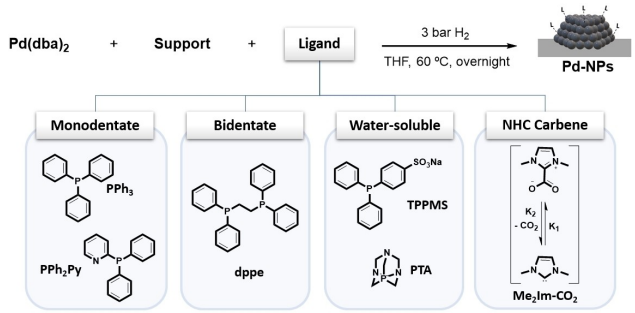

Scheme 1. General procedure for the synthesis of Pd-NPs in the presence of ligands.

Table 1. Characterization data for TiO_2 supported Pd NPs stabilized by different ligands.

Entry	Ligand	Particle size [nm]	ICP [Pd wt%]
1	PPh_3	2.37 ± 0.19	3.98
2	PPh_2Py	2.47 ± 1.30	3.07
3	PTA	1.92 ± 0.91	2.97
4	TPPMS	2.02 ± 1.57	2.99
5	$Me_2Im–CO_2$	2.83 ± 1.38	3.12
6	dppe	2.31 ± 0.82	3.00
7[a]	–	5.36 ± 2.83	4.09
8[b]	PPh_3	2.25 ± 0.91	3.31

Synthesis conditions: Pd 4 wt% (metal precursor $Pd(dba)_2$), 0.2 eq. of ligand (except for dppe and NHC: 0.1 equiv. and 0.5 equiv.), 1 g of TiO_2, 200 ml THF, 3 bar H_2, 60 °C, overnight. [a] In absence of ligand. [b] Using 0.4 eq. of ligand per Pd.

In all cases, highly crystalline small nanoparticles with spherical shape were obtained. In the presence of ligands, the size of the nanoparticles was in the range 2–3 nm with narrow distributions (Table 1, Figure 1). In contrast, when no ligand was used in the synthesis, the nanoparticles displayed a diameter of 5.4 nm with a broad size distribution (Table 1, Entry 7). This clearly indicated the strong stabilizing ability of these ligands and their importance to form small and well-defined NPs under these conditions.

The smallest nanoparticles (*ca.* 2 nm) were obtained using water-soluble phosphines (PTA and TPPMS; Table 1, Entries 3 and 4). Chaudret and co-workers reported the synthesis of Ru and Pt nanoparticles with this ligand and demonstrated that the coordination of PTA to NPs occurs through the P atom.[31] The NPs stabilized with dppe, PPh_3, PPh_2Py and the NHC carbene revealed slightly larger. When the PPh_3:Pd ratio was increased from 0.2 to 0.4 (Entry 1 vs. Entry 8), no significant differences were observed in terms of mean diameter, although the distribution was slightly broader. In terms of metal content, the particles stabilized with PTA and TPPMS have the lowest Pd content and those synthesized in the absence of ligand, the largest.

The presence of the P-based ligands at the surface of the nanoparticles was confirmed by EDX and XPS (Figures 1(c), S5 and S6). XPS analysis of the Pd nanoparticles stabilized with PPh_3 (Figures S3 and S6) also evidenced that mainly zero valent Pd was present at the surface of both colloidal and TiO_2-supported NPs, although some $Pd^{\delta+}$ was detected (16 and 12.5%, respectively). Using reported methods, the percentage of $Pd^{\delta+}$ at the NP surface was calculated to be ca. 20% (Tables S1 and S2).[32,33,34]

XRD analysis did not reveal information about the crystalline structure of the supported nanoparticles due to the high crystallinity of the TiO_2 support and the small size of the nanoparticles (Figure 2(a)). When XRD analysis of the corresponding colloidal nanoparticles was performed, the diffraction pattern observed indicated fcc packing of the Pd NPs in all cases (Figure 2(b)).

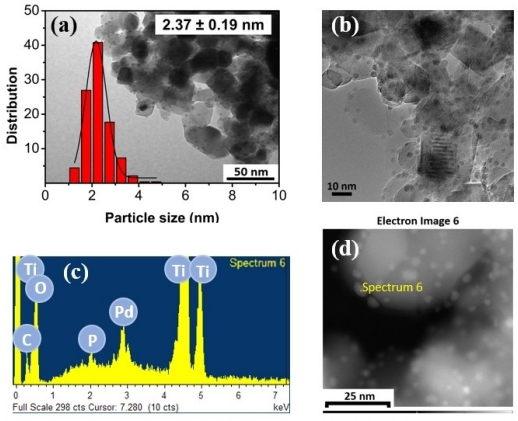

Figure 1. TEM image (a), HR-TEM (b), SEM-EDX (c) and HR-HAADF STEM analysis (d) of the catalyst Pd-PPh_3/TiO_2.

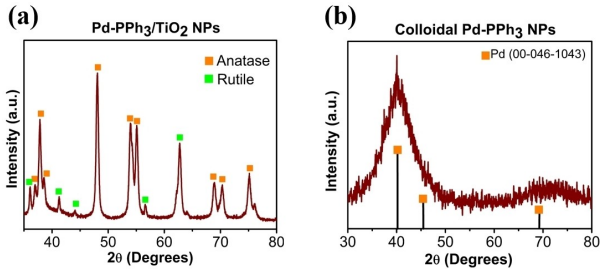

Figure 2. DRX of the catalyst Pd-PPh_3/TiO_2 (a) and colloidal Pd-PPh_3 NPs (b).

Therefore, with this methodology, a series of small and well defined ligand capped Pd NPs supported on TiO_2 was obtained. The presence of the ligands clearly influenced the size and size distribution of the synthesized nanoparticles. Moreover, the steric and electronic properties of these ligands also affected the size of the resulting NPs, although to a smaller extent.

Next, a second series of catalysts was synthesized using different supports such as metal oxides (TiO_2, CeO_2, Al_2O_3) and carbon-based supports (COF TpPa-1, *g*-C_3N_4 and CNTs) using PPh_3 as stabilizing ligand. In all cases, small and highly crystalline nanoparticles with spherical shape were obtained. The mean diameters of the corresponding Pd NPs varied between 2.3 and 3.5 nm depending on the support. When CNTs, COF TpPa-1, TiO_2, CeO_2 and Al_2O_3 were used, the diameter of the resulting Pd NPs was in the range 2–3 nm, while slightly bigger nanoclusters were formed using carbon nitride. Interestingly, previous reports on Pd NPs supported onto COF TpPa-1 described the formation of particles with a diameter of 7 ± 3 nm.[35] Here, in the presence of PPh_3, the size of the NPs obtained onto the same support was *ca.* 2.3 nm, thus again indicating that the use of ligands leads to the formation of smaller and better defined Pd catalysts.

ICP analysis (Table 2) revealed a metal content of 2.09% for the COF TpPa-1 supported catalyst while the TiO_2 based material exhibited a content very close to the nominal value (3.98%). The two supports with the lowest metal content were organic in nature.

Therefore, a strong effect of the support on the size of the Pd NPs was observed, probably due to the strength of the corresponding metal-support interactions.

Table 2. Characterization data for Pd NPs stabilized by PPh_3 onto various supports.

Entry	Support	Particle size [nm]	ICP [Pd wt%]
1	TiO_2	2.37 ± 0.19	3.98
2	CeO_2	2.69 ± 1.28	2.33
3	Al_2O_3	2.95 ± 1.10	3.32
4	CNTs	2.27 ± 1.18	2.55
5	COF TpPa-1	2.33 ± 1.19	2.09
6	*g*-C_3N_4	3.51 ± 0.27	3.07
7[a]	–	1.90 ± 0.57	–

Synthesis conditions: Pd 4 wt% (metal precursor $Pd(dba)_2$), 0.2 eq. of the corresponding ligand, 1 g of corresponding support, 200 ml THF, 3 bar H_2, 60 °C, overnight. [a] In absence of support.

Hydrogenation of CO_2 into formate

Initial catalytic experiments were carried out at 80 °C in water with 4 M $KHCO_3$ and a total pressure of 36 bar ($CO_2/H_2 = 1$) using both sets of synthesized Pd NPs as catalysts.

The results obtained using TiO_2 supported catalysts bearing various ligands are summarized in Table 3.

The turnover numbers obtained varied from 385 for the PTA capped catalyst (Entry 3) up to 876 (Entry 1) for that synthesized in the presence of PPh_3. It is noteworthy that when the catalytic experiments were performed using the catalysts synthesized in the presence of 0.4 eq. of PPh_3, the activity remained practically unchanged (Entry 8). The catalysts stabilized by the bidentate ligand dppe also provided high catalytic activity (TON = 856) while those containing PPh_2Py and TPPMS presented intermediate catalytic activities (TON = ca. 700, entries 2 and 4). Nanoparticles without ligand and those stabilized with NHC provided TON values somewhat lower (Entries 5 and 6).

Based on these results, it can be concluded that the catalytic activity is not directly related with the size of the NPs (Figure 3) since the smallest NPs (PTA) provided the lowest TON value while the largest NPs (synthesized in the absence of ligand) exhibited an intermediate activity. In this series, the most active catalysts were those stabilized by PPh_3 and dppe. Recently, Staiger et al.[36] used different phosphines as additives for the synthesis of colloidal Pd NPs for semi-hydrogenation of alkynes. In their case, the results with PPh_3, compared with bulkier phosphines, provided the highest catalytic selectivity, which was explained by the steric inhibition of the active sites at the particle surface.

Table 3. Effect of the ligand in CO_2 hydrogenation to formate.[a]

Entry	Ligand	TON[b]	TOF [h^{-1}][c]
1	PPh_3	876	58
2	PPh_2Py	700	47
3	PTA	385	26
4	TPPMS	701	47
5	Me_2Im–CO_2	506	34
6	Without	572	38
7	dppe	856	57
8	PPh_3 (0.4 eq.)	868	58

[a] 20 mg of Palladium nanoparticles supported over TiO_2 catalyst stabilized with different ligands, 5 ml H_2O milli-Q, $KHCO_3$ (4 M), 80 °C, pTotal = 36 bar, $p(CO_2) = p(H_2)$, t = 15 h. [b] TON = mmol formate/mmol total of Pd, calculated by NMR using 1,4-dioxane as internal standard. [c] TOF = TON/t(h).

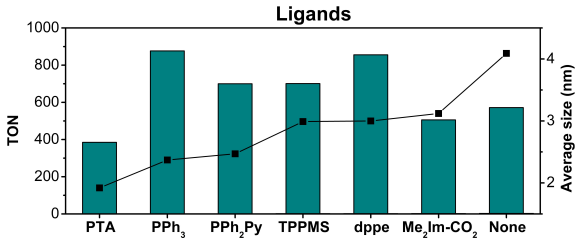

Figure 3. Effect of the ligand on the size of NPs and catalytic activity for the hydrogenation of CO_2.

It should be noted that low catalytic activity was obtained using the NPs stabilized with NHC ligand, which could be due the stronger interaction between Pd and the ligand that reduced the number of active sites during catalysis. In the ligand-free nanoparticles, despite a more available surface, the activity was lower compared to most catalysts stabilized by phosphine ligands, which could be attributed to the size of the NPs or some electronic effect induced by the ligands. Surprisingly, when the nanoparticles containing PTA, which exhibited the smallest size, were used, the lowest catalytic activity was obtained. This could be due to the blocking of surface active sites by the ligand and/ or a fast catalyst deactivation. For other water-soluble ligand (TPPMS) the activity was higher. For PPh_2Py, the catalytic activity was very similar to that of TPPMS.

Therefore, the variations observed in catalytic activity could not be related with the size of the nanoparticles obtained during the catalyst preparation, but with the electronic and steric properties that the ligands confer to the active phase.

Next, the effect of the support was evaluated in the CO_2 hydrogenation to formate under basic conditions. The results are summarized in Table 4.

Among the series, the highest activity was obtained using the TiO_2-based catalyst (Table 4, Entries 1). All the other supports provided much lower activities. For other metal oxides such as Al_2O_3, the TON values were below 300 (Entries 2 and 4). In the case of carbon-based supports, the highest activity was achieved using *g*-C_3N_4 (TON = 465, entry 6), followed by COF TpPa-1 (TON = 321) while very low activity was obtained with catalysts supported on CNTs and colloidal nanoparticles.

Comparing the results obtained with metal oxides, these results are in agreement with a previous report by Mori et al.[23] that described that TiO_2 based catalysts were more efficient than those on CeO_2. Regarding the size of the nanoparticles, in these two catalysts (2.37 ± 0.19 nm vs. 2.69 ± 1.28 nm, Figure 4, Figure S4 and Table 2), values are similar. However, the metal content was higher (3.98 ± 0.03 wt% Pd) for Pd/TiO_2 than for Pd/CeO_2 (2.33 wt%), which could indicate a stronger metal-support interaction between Pd and TiO_2. Within the series, the lowest activity was observed for the Pd/COF TpPa-1 system (Table 4, Entry 5). This result could be explained by some stability issue of this support under basic conditions, as previously described,[37] although in another report, Pd catalysts supported on COF TpPa-1 were previously reported and no stability issues were indicated.[35]

These results thus highlight the importance of metal-support interactions to reach high catalytic activity in this reaction.

As previously mentioned, the base plays a fundamental role in the thermodynamics of this process. At pH 6–9, the true substrate of the reaction is not CO_2, but bicarbonate (HCO_3^-) since CO_2 dissolved in water shows a pH-dependent equilibrium between the HCO_3^- species (pKa1 = 6.35 at 25 °C) and CO_3^{2-} (pKa2 = 10.33).[38] It was previously reported that the hydrogenation of carbonates is more difficult than that of bicarbonates in aqueous solutions.[18c] Consequently, by increasing the pH, the balance changes from bicarbonate to carbonate, thus decreasing the yield to formate. Furthermore, the pH of the solution can influence the stability of metal hydrides.[39]

In this study, various organic and inorganic bases such as NEt_3, KOH, $KHCO_3$ and $NaHCO_3$ were tested (Table 5 and Figure 5). In the absence of base (Table 5, Entry 5), hardly any catalytic activity was observed. When NEt_3 was used (Table 5, Entry 4), low activity was obtained, probably due to the low

Table 4. Effect of the support in CO_2 hydrogenation to formate.[a]

Entry	Support	TON[b]	TOF [h^{-1}][c]
1	TiO_2	876	58
2	CeO_2	243	16
3	CNTs	15	–
4	Al_2O_3	284	19
5	COF TpPa-1	321	21
6	*g*-C_3N_4	465	31
7	*Unsupported*	7	–

[a] 20 mg of Palladium supported nanoparticles catalyst stabilized with PPh_3, 5 ml H_2O milli-Q, $KHCO_3$ (4 M), 80 °C, pTotal = 36 bar, $p(CO_2) = p(H_2)$, t = 15 h. [b] TON = mmol formate/mmol total of Pd, calculated by NMR using 1,4-dioxane as internal standard. [c] TOF = TON/t(h).

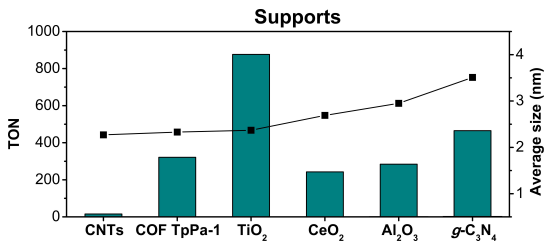

Figure 4. Effect of the support in the catalytic activity as a function of NP size for the hydrogenation of CO_2.

Table 5. Effect of the nature of the base in CO_2 hydrogenation to formate.[a]

Entry	Base, 1 M	TON[b]	TOF [h^{-1}][c]
1	$NaHCO_3$	242	16
2	$KHCO_3$	319	21
3	KOH	229	15
4	NEt_3	6	0.4
5	None	9	0.6

[a] 20 mg Pd-PPh_3/TiO_2 NPs, 5 ml H_2O milli-Q, 80 °C, pTotal = 36 bar, $p(CO_2) = p(H_2)$, 15 h. [b] TON = mmol formate/mmol total of Pd, calculated by NMR using 1,4-dioxane as internal standard. [c] TOF = TON/t(h).

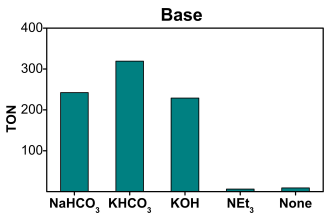

Figure 5. Effect of the base in the catalytic activity for the hydrogenation of CO_2. Conditions: 20 mg Pd-PPh_3/TiO_2 NPs, 5 ml H_2O milli-Q, base (1 M), 80 °C, pTotal = 36 bar, $p(CO_2) = p(H_2)$, 15 h. TON = mmol formate/mmol total of Pd, calculated by NMR using 1,4-dioxane as internal standard.

solubility of this base in the reaction medium. When bicarbonates were used, high catalytic activity was reached with $KHCO_3$ compared with that obtained with $NaHCO_3$ (Table 5, Entry 2 vs. Entry1). Similar effect was previously reported.[38] Indeed, the cation can affect the balance between carbonate and bicarbonate. Moreover, $KHCO_3$ provides a higher concentration of HCO_3^- than $NaHCO_3$ in solution.[40,11c,18c] Using KOH, (Table 5, Entry 3), the catalytic activity was similar to that obtained using $NaHCO_3$.

The concentration of the base also proved important as TON values increased at higher base concentrations (Table S3).

When the reaction temperature was optimized, the highest activity was obtained at 60 °C (Figure 6(c), Table S5, Entry 2). The results described a volcano plot that could be explained by the lower solubility of CO_2 at higher temperature and/or the lower stability of the catalysts at T > 60 °C. In terms of total pressure, upon increasing from 9 to 18, 24 up to 36 bar of CO_2, (Figure 6(a) and Table S6), the catalytic activity continuously increased. In terms of partial pressures (Figure 6, Table S7), the ratio pCO_2:pH_2 1:2 (Entry 3) provided the highest activity with a TON value of 1145.

When the reaction was monitored over time (Figure 6(d), Table S8), the TON values remained constant after 15 h of reaction, indicating deactivation of the catalyst.

Reusability of catalyst

A recyclability experiment was performed under optimized conditions using the TiO_2-supported Pd catalysts synthesized in the presence of PPh_3. After each catalytic test, the catalyst was recovered by centrifugation, washed three times with Milli-Q water and dried. Then, the catalyst was redispersed in water, and fresh $KHCO_3$ and 1,4-dioxane were added. The procedure was repeated three times. However, a decrease in catalytic activity was observed after each run. TEM images of the catalyst (Figure 7(b) and 7(c)) after the third recovery revealed that the NPs had considerably increased in size (ca. 6 nm) and in some regions, agglomeration was also detected. Similar results were reported by Mori et al. for the system $PdAg/TiO_2$.[41] To avoid such agglomerations in catalysis, the use of ligands, polymers or surfactants were previously reported.[42] ICP measurements of the catalytic solutions were performed but no Pd could be detected, indicating that no Pd leaching had occurred. It was therefore concluded that sintering of the Pd NPs was responsible of the decrease in catalytic activity during these experiments.

Conclusions

In this work, novel catalysts based on ligand-capped Pd NPs supported on various materials were prepared and their activity was evaluated in the hydrogenation of CO_2 to formate. The results revealed the importance of the ligand in obtaining small and well defined catalysts, although the size of the nanoparticles could not be directly correlated with their catalytic performance and the interactions between the nanoparticles and the support appeared to be critical to the catalyst activity. The Pd-PPh_3/TiO_2 catalytic system reached a TON of 1032 (TOF of 69 h^{-1}, [HCOOK] = 1.1 mol/l) under mild conditions of pressure and temperature (36 bar ($pCO_2 = pH_2$), 60 °C, 15 h). Initial recycling study revealed unsuccessful and current efforts are focused on support modification to limit sintering and enhance catalytic activity of these catalysts.

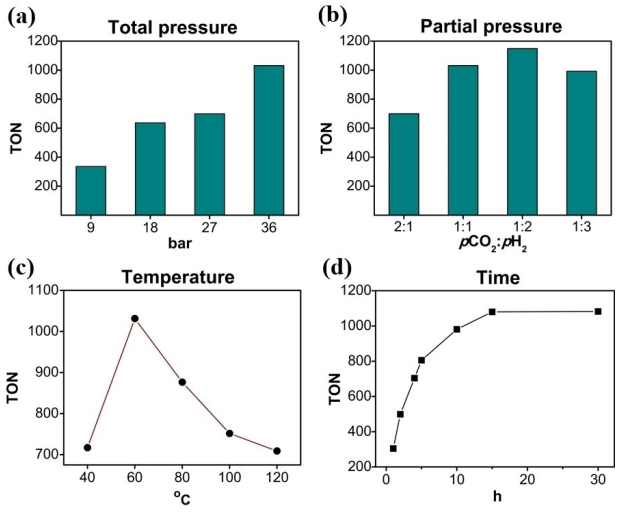

Figure 6. Variation of TON values as a function of (a) total pressure, (b) partial pressures, (c) temperature and (d) time in the hydrogenation of CO_2 using Pd-PPh_3/TiO_2 as catalyst. Conditions: 20 mg Pd-PPh_3/TiO_2 NPs, 5 ml H_2O milli-Q, $KHCO_3$ (4 M). TON = mmol formate/mmol total of Pd, calculated by NMR using 1,4-dioxane as internal standard. TOF = TON/t(h).

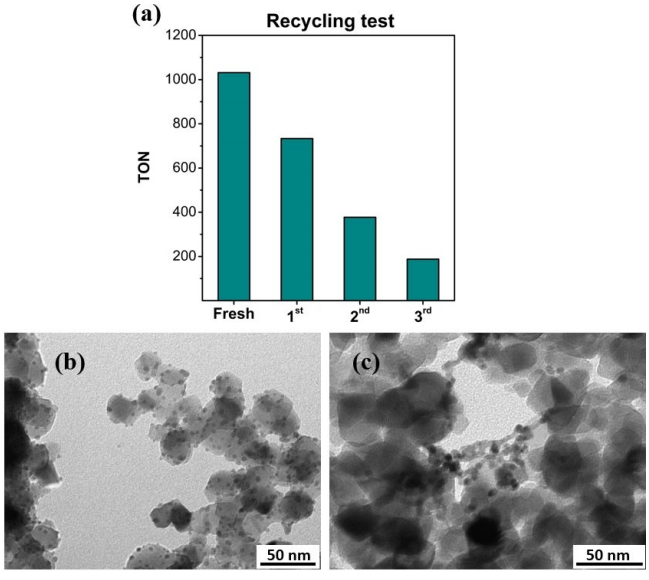

Figure 7. Recycling experiment with the catalyst Pd-PPh_3/TiO_2 (a) and TEM images before catalysis (b) and after catalysis (c) with NPs on the order of 6 nm NPs (b) and agglomerates (c). Conditions: 20 mg of Pd-PPh_3/TiO_2 catalyst, 5 ml H_2O milli-Q, $KHCO_3$ (4 M), pTotal = 36 bar, $p(CO_2) = p(H_2)$, 60 °C. TON = mmol formate/mmol total of Pd, calculated by NMR using 1,4-dioxane as internal standard.

Experimental Section

Synthetic procedures, TEM, XRD, XPS, EDX, HRTEM images and results of catalysis experiment of hydrogenation of CO_2 to formate under different conditions can be found in the Supporting Information. This material is available free of charge via Internet.

Synthesis and characterization of PPh_3 stabilized Pd NPs supported over TiO_2

The catalysts were prepared to obtain a 4% wt Pd loading over TiO_2. TiO_2 was weighted outside the glove box and left in an oven at 100 °C overnight. In a typical experiment, metal precursor and the stabilizer were weighted in the glove box and charged into a Fischer-Porter bottle. At this point, TiO_2 and solvent were added, the Fischer-Porter was closed, purged with hydrogen several times and then charged with 3 bar of H_2. The reaction mixture was left stirring (700 rpm) at 60 °C overnight. After the reaction, Fischer-Porter was cooled at room temperature, depressurized and entered inside glove box. TEM samples were prepared using five drops of the crude solution and depositing onto a copper grid. The rest of the reaction crude was concentrated and washed several times with hexane. The catalyst was dried under vacuum during several hours.

Catalytic experiments for CO_2 reduction to formate

Stainless steel high-pressure reactor HEL CAT-7 (7×10 ml) was charged with TiO_2 supported palladium nanoparticles (20 mg), 20 mg of 1,4-dioxane and 5 ml of a 4 M base solution employing Milli-Q water. The reactor was first flushed with 3 cycles of hydrogen to remove the air. Then, the reactor was charged with 10 bar of H_2 and heated at 40 °C under stirring for twenty minutes. At this point, the reactor was depressurized, purged several times with CO_2 and charged with 18 bar of CO_2 and let under stirring for 20 minutes. Then, the reactor was charged with 18 bar of H_2 (1:1, CO_2:H_2) and heated to reach the temperature under 600 rpm of stirring. The experiment was left 15 h and after this time, the reactor was allowed to cool in an ice bath. When the reactor was cooled, it was depressurized and opened. A small amount of the sample was filtered through celite and analysed by NMR using D_2O as deuterated solvent.

Acknowledgements

The authors are grateful to the Spanish Ministerio de Ciencia e Innovación (CTQ2016-75016-R and PID2019-104427RB-I00) and the Generalitat de Catalunya (2021SGR00163) for financial support and the FPI grant (BES-2017-081305). Authors also thank the Servei of Recursos Cientifics i Tecnics of Universitat Rovira i Virgili for the analytical assistance, to the Advanced Microscopy Laboratory at Instituto de Nanociencia of the Universidad of Zaragoza for the HRTEM and STEM experiments, Fundació Institut Català de Nanociència i Nanotecnologia (ICN2) for XPS experiments. Authors are also grateful to Dr. Aitor Gual for his help with XPS data.

Conflict of Interest

The authors declare no conflict of interest.

Data Availability Statement

The data that support the findings of this study are available in the supplementary material of this article.

Keywords: CO_2 hydrogenation · ligand stabilizer · nanoparticles · palladium · supported catalyst

[1] a) G. Centi, S. Perathoner, *Catal. Today* **2009**, *148*, 191–205; b) G. Centi, E. A. Quadrelli, S. Perathoner, *Energy Environ. Sci.* **2013**, *6*, 1711–1731; c) A. Dibenedetto, A. Angelini, P. Stufano, *J. Chem. Technol. Biotechnol.* **2014**, *89*, 334–353.
[2] P. Styring, D. Jansen, H. de Coninck, H. Reith, K. Armstrong, *Carbon Capture and Utilisation in the green economy*, Centre for Low Carbon Futures, **2011**, http://co2chem.co.uk/carbon-captureand-utilisation-in-the-green-economy.
[3] S. Ghazali-Esfahani, H. Song, E. Păunescu, F. D. Bobbink, H. Liu, Z. Fei, G. Laurenczy, M. Bagherzadeh, N. Yan, P. J. Dyson, *Green Chem.* **2013**, *15*, 1584–1589.
[4] E. Alper, O. Yuksel Orhan, *Petroleum* **2017**, *3*, 109–126.
[5] M. Kurtz, N. Bauer, C. Büscher, H. Wilmer, O. Hinrichsen, R. Becker, S. Rabe, K. Merz, M. Driess, R. A. Fischer, M. Muhler, *Catal. Lett.* **2004**, *92*, 49–52.
[6] S. Vukojevic, O. Trapp, J.-D. Grunwaldt, C. Kiener, F. Schüth, *Angew. Chem. Int. Ed.* **2005**, *44*, 7978–7981; *Angew. Chem.* **2005**, *117*, 8192–8195.
[7] C. He, G. Tian, Z. Liu, S. Feng, *Org. Lett.* **2010**, *12*, 649–651.
[8] S. Wesselbaum, V. Moha, M. Meuresch, S. Brosinski, K. M. Thenert, J. Kothe, T. V. Stein, U. Englert, M. Holscher, J. Klankermayer, W. Leitner, *Chem. Sci.* **2015**, *6*, 693–704.
[9] M. Siebert, M. Seibicke, A. F. Siegle, S. Kräh, O. Trapp, *J. Am. Chem. Soc.* **2019**, *141*, 334–341.
[10] M. Ni, M. K. H. Leung, D. Y. C. Leung, K. Sumathy, *Renewable Sustainable Energy Rev.* **2007**, *11*, 401–425.
[11] a) J. Ohi, *J. Mater. Res.* **2005**, *20*, 3180–3187; b) J. H. Lee, J. Ryu, J. Y. Kim, S.-W. Nam, J. H. Han, T.-H. Lim, S. Gautam, K. H. Chaec, C. W. Yoon, *J. Mater. Chem. A* **2014**, *2*, 9490–9495;c) J. H. Lee, J. Ryu, J. Y. Kim, S.-W. Nam, J. H. Han, T.-H. Lim, S. Gautam, K. H. Chaec, C. W. Yoon, *J. Mater. Chem. A* **2014**, *2*, 9490–9495; d) H. Zhong, M. Iguchi, M. Chatterjee, T. Ishizaka, M. Kitta, Q. Xu, H. Kawanami, *ACS Catal.* **2018**, *8*, 5355–5362;
[12] P. Upadhyay, V. Srivastava, *PESD* **2016**, *10*, 13–34.
[13] J. Klankermayer, S. Wesselbaum, K. Beydoun, W. Leitner, *Angew. Chem. Int. Ed.* **2016**, *55*, 7296–7343; *Angew. Chem.* **2016**, *128*, 7416–7467.
[14] a) G. H. Gunasekar, J. Shin, K.-D. Jung, K. Park, S. Yoon, *ACS Catal.* **2018**, *8*, 4346–4353; b) Z. Zhang, Y. Xie, W. Li, S. Hu, J. Song, T. Jiang, B. Han, *Angew. Chem.* **2008**, *120*, 1143–1145; *Angew. Chem. Int. Ed.* **2008**, *47*, 1127–1129; c) H.-K. Lo, C. Copéret, *ChemCatChem* **2019**, *11*, 430–434.
[15] a) R.-P. Ye, J. Ding, W. Gong, M. D. Argyle, Q. Zhong, Y. Wang, C. K. Russell, Z. Xu, A. G. Russell, Q. Li, M. Fan, Y.-G. Yao, *Nat. Commun.* **2019**, *10*, 5698; b) D. Preti, C. Resta, S. Squarcialupi, G. Fachinetti, *Angew. Chem. Int. Ed.* **2011**, *50*, 12551–12554; *Angew. Chem.* **2011**, *123*, 12759–12762; c) C. Hao, S. Wang, M. Li, L. Kang, X. Ma, *Catal. Today* **2011**, *160*, 184–190; d) D. A. Bulushev, J. R. H. Ross, *Catal. Rev. Sci. Eng.* **2018**, *60*, 566–593.
[16] a) L. Fan, Y. Sakaiya, K. Fujimoto, *Appl. Catal. A* **1999**, *180*, L11-L13; b) A. García-Trenco, A. Regoutz, E. R. White, D. J. Payne, M. S. P. Shaffer, C. K. Williams, *Appl. Catal. B* **2018**, *220*, 9–18.
[17] a) K. Zhou, Y. Li, *Angew. Chem. Int. Ed.* **2012**, *51*, 602–613; *Angew. Chem.* **2012**, *124*, 622–635; b) L. I. Zhang, M. X. Zhou, A. Q. Wang, T. Zhang, *Chem. Rev.* **2019**, *120*, 683–733.
[18] a) H. Park, J. H. Lee, E. H. Kim, K. Y. Kim, Y. H. Choi, D. H. Younb, J. S. Lee, *Chem. Commun.* **2016**, *52*, 14302–14305; b) X. Shao, X. Miao, X. Yu, W. Wang, X. Ji, *RSC Adv.* **2020**, *10*, 9414–9419; c) J. Su, M. Lu, H. Lin, *Green Chem.* **2015**, *17*, 2769–2773; d) W.-H. Wang, X. Feng, M. Bao, *Transformation of CO_2 to Formic Acid or Formate Over Heterogeneous Catalysts*, chapter 3, 2017, 43–52, Online ISBN 978-981-10-3250-9.
[19] K. Nakajima, M. Tominaga, M. Waseda, H. Miura, T. Shishido, *ACS Sustainable Chem. Eng.* **2019**, *7*, 6522–6530.
[20] a) Y. Kuwahara, Y. Fujie, T. Mihogi, H. Yamashita, *ACS Catal.* **2020**, *10*, 6356–6366; b) G. Yang, Y. Kuwahara, S. Masuda, K. Mori, C. Louis, H.

Yamashita, *J. Mater. Chem. A* **2020**, *8*, 4437–4446; c) K. Mori, T. Sano, H. Kobayashi, H. Yamashita, *J. Am. Chem. Soc.* **2018**, *140*, 8902–8909.
[21] L. T. M. Nguyen, H. Park, M. Banu, J. Y. Kim, D. H. Youn, G. Magesh, W. Y. Kima, J. S. Lee, *RSC Adv.* **2015**, *5*, 105560–105566.
[22] X. Shao, J. Xu, Y. Huang, X. Su, H. Duan, X. Wang, T. Zhang, *AIChE J.* **2016**, *62*, 2410–2418.
[23] K. Mori, T. Sano, H. Kobayashi, H. Yamashita, *J. Am. Chem. Soc.* **2018**, *140*, 8902–8909.
[24] K. Philippot, B. Chaudret, *C. R. Chim.* **2003**, *6*, 1019–1034.
[25] A. Balanta, C. Godard, C. Claver, *Chem. Soc. Rev.* **2011**, *40*, 4973–4985.
[26] Y. Zhang, J. Feia, Y. Yua, X. Zheng, *Catal. Lett.* **2004**, *93*, 231–234.
[27] a) W. Zhang, S. Wang, Y. Zhao, X. Ma, *Fuel Process. Technol.* **2018**, *178*, 98–103; b) V. Srivastava, *Catal. Lett.* **2014**, *144*, 2221–2226; c) P. R. Upadhyay, V. Srivastava, *RSC Adv.* **2016**, *6*, 42297–42306; d) Z.-Z. Yang, H. Zhang, B. Yu, Y. Zhao, G. Ji, Z. Liu, *Chem. Commun.* **2015**, *51*, 1271–1274; e) S. Wang, S. Hou, C. Wu, Y. Zhao, X. Ma, *Chin. Chem. Lett.* **2019**, *30*, 398–402.
[28] a) S. Wesselbaum, U. Hintermair, W. Leitner, *Angew. Chem.* **2012**, *124*, 8713–8716; *Angew. Chem. Int. Ed.* **2012**, *51*, 8585–8588; b) P. G. Jessop, F. Joó, C.-C. Tai, *Coord. Chem. Rev.* **2004**, *248*, 2425–2442; S. Moret, P. J. Dyson, G. Laurenczy, *Nat. Commun.* **2014**, *5*, 4017; c) J. Elek, L. Nádasdi, G. Papp, G. Laurenczy, F. Joó, *Appl. Catal. A* **2003**, *255*, 59–67.
[29] K. J. Fisher, E. C. Alyea, N. Shahnazarian, *Phosphorus, Sulfur, Silicon Relat. Elem.* **1990**, *48*, 37–40.
[30] a) M. Díaz de los Bernardos, S. Pérez-Rodríguez, A. Gual, C. Claver, C. Godard, *Chem. Commun.* **2017**, *53*, 7894–7897; b) D. A. Lomelí-Rosales, J. A. Delgado, M. Díaz de los Bernardos, S. Pérez-Rodríguez, A. Gual, C. Claver, C. Godard, *Chem. Eur. J.* **2019**, *25*, 8321–8331.
[31] P.-J. Debouttière, Y. Coppel, A. Denicourt-Nowicki, A. Roucoux, B. Chaudret, K. Philippot, *Eur. J. Inorg. Chem.* **2012**, 1229–1236.
[32] C. Rangheard, C. de Julián Fernández, P.-H. Phua, J. Hoorn, L. Lefort, J. G. de Vries, *Dalton Trans.* **2010**, *39*, 8464–8471.
[33] B. K. Teo, N. J. A. Sloane, *Inorg. Chem.* **1985**, *24*, 4545–4558.
[34] V. Hardevel, V. Hartog, *Surf. Sci.* **1969**, *15*, 189–230.
[35] P. Pachfule, M. K. Panda, S. Kandambeth, S. M. Shivaprasad, D. D. Díaz, R. Banerjee, *J. Mater. Chem. A* **2014**, *2*, 7944–7952.
[36] L. Staiger, T. Kratky, S. Günther, O. Tomanek, R. Zbořil, R. W. Fischer, R. A. Fischer, M. Cokoja, *ChemCatChem* **2021**, *13*, 227–234.
[37] S. Kandambeth, A. Mallick, B. Lukose, M. V. Mane, T. Heine, R. Banerjee, *J. Am. Chem. Soc.* **2012**, *134*, 19524–19527.
[38] T. Wang, D. Ren, Z. Huo, Z. Song, F. Jin, M. Chen, L. Chen, *Green Chem.* **2017**, *19*, 716–721.
[39] J. Sá, G. D. Arteaga, R. A. Daley, J. Bernardi, J. A. Anderson, *J. Phys. Chem. B* **2006**, *110*, 17090–17095.
[40] J. Su, L. Yang, M. Lu, H. Lin, *ChemSusChem* **2015**, *8*, 813–816.
[41] K. Mori, A. Konishi, H. Yamashita, *J. Phys. Chem. C* **2020**, *124*, 11499–11505.
[42] M. T. Reetz, W. Helbig, S. A. Quaiser, U. Stimming, N. Breuer, R. Vogel, *Science* **1995**, *267*, 367–369.

Manuscript received: November 15, 2022
Revised manuscript received: January 13, 2023
Accepted manuscript online: January 18, 2023
Version of record online: February 2, 2023